Phase Angle Effects on Fracture Toughness of Polymer Interfaces Reinforced with Block Copolymers

Fei Xiao and Chung-Yuen Hui*

Department of Theoretical and Applied Mechanics and the Materials Science Center, Cornell University, Ithaca, New York 14853

Junichiro Washiyama† and Edward J. Kramer

Department of Materials Science and Engineering and the Materials Science Center, Cornell University, Ithaca, New York 14853

Received January 5, 1994®

ABSTRACT: The effect of the phase angle ψ on fracture toughness and fracture mechanisms of planar interfaces between polystyrene (PS) and poly(2-vinylpyridine) (PVP) reinforced with deuterium-labeled polystyrene (dPS)/PVP block copolymers was investigated using an asymmetric double cantilever beam (ADCB) specimen. The fracture toughness of an interfacial crack, G_c, was measured as a function of the phase angle ψ, the areal chain density of the block copolymer Σ, and the degree of polymerization N of the chains. The fracture mechanisms of the interface were studied by forward recoil spectrometry (FRES), which permitted the location of the dPS block to be determined after fracture. There is a dramatic change in fracture toughness as the phase angle changes sign, a change which is associated with the formation of crazes in the PS at, and away from, the interface. The angle θ of craze propagation away from the interface depends on the phase angle ψ. For positive phase angles, θ is close to 45°; for negative phase angles, θ is close to 135°.

1. Introduction

Block copolymers have been widely used to reinforce interfaces between immiscible polymers.[1,2] The reinforcement mechanism is believed to be "stitching"; i.e., block copolymer chains form interphase junctions through which stress can be transferred, which results in substantial reinforcement of the interfaces. Creton et al.[3] examined this reinforcing effect of dPS/PVP block copolymers and concluded that at least one entanglement between each block and its respective homopolymer was necessary to achieve effective interfacial reinforcement.

The reinforcement effect of block copolymers was measured by the fracture toughness increases of the PS/PVP interfaces. Recently, an asymmetric double cantilever beam specimen has been developed[4,5] and applied to measure the fracture toughness of interfaces between immiscible polymers and the interfaces between polymer and nonpolymer materials[6–9] (Figure 1). In these studies, it was found that changing the thickness ratio of the two beams in the ADCB specimen results in significant changes in the measured fracture toughness of the same interface.[3,7–9] In some cases, the crack can be driven out of the interface by changing the thickness ratio, resulting in cohesive failure of PS or PVP instead of adhesive failure along the interface. Changing the thickness ratio changes the phase angle ψ which controls the ratio of the shear/normal traction directly ahead of the interface crack tip. To quantify the improvement in the fracture toughness of the interfaces as a function of polymerization index of both blocks, N_{PS} and N_{PVP}, and the areal density of the block copolymer chains, Σ, our previous experiments[7,8,10] were conducted with a fixed phase angle of about −6°, which corresponds to a fixed PS/PVP thickness ratio of 2.3/1.6, so the crack remains on the interface as it is driven toward the more craze resistant PVP. The objective of this work is to determine the dependence of interface fracture toughness G_c on the phase angle ψ and how that dependence is altered when Σ and the polymerization indices of the block copolymer are changed.

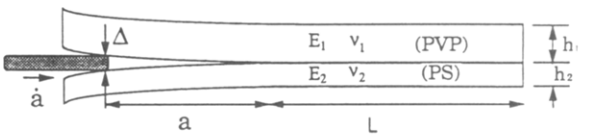

Figure 1. ADCB specimen with PVP as the top beam.

As in previous experiments, we chose polystyrene (PS) and poly(2-vinylpyridine) (PVP) homopolymers as the immiscible polymer pair and dPS/PVP block copolymers to reinforce the interface between PS and PVP. There are several advantages of this system. Both PS and PVP deform plastically by crazing,[7] which can be investigated using transmission electron microscopy (TEM) techniques.[11] The PS phase has a smaller crazing stress than PVP, so it will craze before PVP does. Furthermore, thermodynamic characteristics, such as the Flory interaction parameter, χ, between PS and PVP are known from previous studies,[12–14] giving us an additional advantage in understanding this system.

According to the deformation–fracture mechanism map proposed by Xu et al.[15] and Washiyama et al.,[8] two transitions of fracture mechanism are possible as Σ increases. The first, for long blocks (i.e., both N_{PS} and $N_{PVP} \gg N_e$, where N_e denotes the polymerization index between entanglements of its respective homopolymer[7]), is the transition from chain scission (with negligible crazing) to crazing (followed by chain scission in the craze). The second is the transition from chain pull-out to crazing (e.g., when $N_{PVP} < N_e$ for the PVP block).[8]

2. Fracture Mechanics

The mechanics of fracture along a bimaterial interface has been studied extensively. Excellent reviews can be found in refs 4, 7, 9, and 16–22.

The stress and deformation field near the tip of a crack lying along a bimaterial interface can be uniquely characterized by the complex stress intensity factor $K = K_1 + iK_2$,[19] $i = (-1)^{1/2}$. K_1 and K_2 have dimensions of (Pa m$^{1/2-i\epsilon}$)

† Visiting scientist from Kawasaki Plastics Laboratory, Showa Denko K.K., 3-2 Chidori-cho, Kawasaki-ku, Kawasaki, Kanagawa 210, Japan.

® Abstract published in *Advance ACS Abstracts,* June 1, 1994.

0024-9297/94/2227-4382$04.50/0

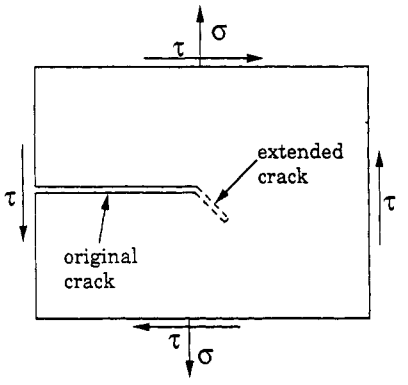

Figure 2. Possible crack kinking extension direction in a K field with $\psi > 0$ for the case $\epsilon = 0$.

and are functions of the sample geometry, applied loading, and material properties. In experiments, it is easier to measure the energy release rate G, which is related to K by

$$G = C|K|^2/[16\cosh^2(\pi\epsilon)] \quad (1)$$

where

$$\epsilon = (1/2\pi)\ln[(\kappa_1/\mu_1 + 1/\mu_2)/(\kappa_2/\mu_2 + 1/\mu_1)] \quad (2a)$$

$$C = (\kappa_1 + 1)/\mu_1 + (\kappa_2 + 1)/\mu_2 \quad (2b)$$

$\kappa_i = 3 - 4\nu_i$ for plane strain and $(3 - \nu_i)/(1 + \nu_i)$ for plane stress. ν_i and μ_i are Poisson's ratio and the shear modulus of material i. For the PVP/PS system, the shear moduli and Poisson's ratios for the two materials are $\mu_2 = \mu_{PS} = 1.119$ GPa, $\nu_2 = \nu_{PS} = 0.341$, $\mu_1 = \mu_{PVP} = 1.321$ GPa, and $\nu_1 = \nu_{PVP} = 0.325$. ϵ is found to be -2.8×10^{-3} for interfaces under plane strain conditions.

Since G is real, an additional dimensionless quantity, the phase angle ψ, is needed to fully specify the crack tip field. ψ is defined by

$$\exp(i\psi) = (Kd^{i\epsilon})/|K| \quad (3)$$

The choice of the characteristic length d is arbitrary (see ref 19). For the PVP/PS system, d is chosen to be 100 μm, which is outside of the craze zone ahead of the crack tip.[23] Note that, for the special case of a homogeneous material, $\epsilon = 0$, K_1 and K_2 become the classical tensile and shear stress intensity factors K_I and K_{II}. In this case, ψ is the tensile and shear mode mixity at the crack tip; i.e., $\psi = \tan^{-1}(K_{II}/K_I)$. Figure 2 shows the stress state near the crack tip corresponding to the case $\psi > 0$. In this case, the crack has a tendency to deflect into the lower half plane following the $\sigma_{r\theta} = 0$ direction in the K field.

The development of a test specimen for measuring interface fracture toughness involves finding analytical or numerical solutions for G and ψ. G and ψ for the ADCB specimen used in our experiments were computed using a boundary element method which was reported in ref 23.

3. Experimental Methods

3.1. Materials. PS and PVP homopolymers purchased from Aldrich Chemical Co. Inc. were of commercial grade with weight-average molecular weights of 250 000 and 200 000, respectively. The deuterated polystyrene/poly(2-vinylpyridine) (dPS/PVP) block copolymer used in this study was synthesized by anionic polymerization in tetrahydrofuran using cumylpotassium as the initiator at −55 °C in an argon atmosphere. The molecular weight and the composition of the block copolymer were characterized using gel permeation chromatography (GPC), forward recoil spectrometry (FRES),[24,25] and nuclear magnetic resonance (NMR). The polymerization indices of the dPS and the PVP blocks, (N_{PS}, N_{PVP}), were (580, 220), (800, 870), and (510, 540), respectively. The polydispersity indices were less than 1.1. Details of the polymerization and the characterization can be found elsewhere.[26] The PS block was deuterium labeled so that the quantity of the PS block at the interface could be analyzed with FRES.

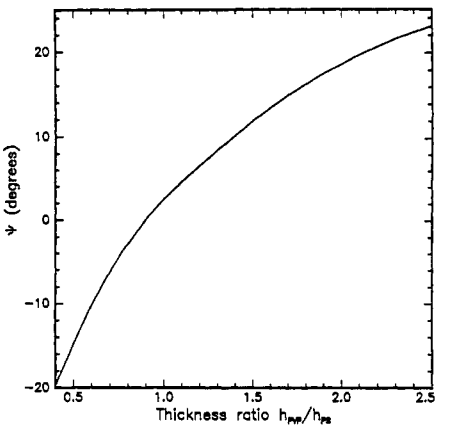

Figure 3. Relationship between h_{PVP}/h_{PS} and phase angle ψ from numerical calculations.

The polymerization indicies of the dPS blocks of all the copolymers used in the experiments reported below are larger than the polymerization index between entanglements, $N_{e;PS}$ (=173), ensuring that the dPS block can form entanglements with the PS homopolymer. On the other hand, the polymerization index of one PVP block is 220, which is smaller than $N_{e;PVP}$ (=255), while those of the other two are greater.

3.2. Sample Preparation. Slabs of PS and PVP were fabricated by compression molding at 160 °C. The thickness of the slab was controlled by the thickness of a metal molding plate frame. The molding plate frame thicknesses were 3.2, 2.3, 2.0, and 1.6 mm. Different combinations of these thicknesses give different phase angles, ranging from −15 to +20°. A thin film of the block copolymer was spun cast from a toluene solution on the PVP slab. The slab was dried at 80 °C, which is well below the glass transition temperature T_g of PVP (108 °C), for 2 h in vacuum. This drying process does not induce the diffusion of block copolymer chains into PVP homopolymer. The areal density of block copolymer chains at the interface, Σ, was controlled by varying the concentration of the block copolymer in solution (0.2–2.5%), which determined in turn the thickness of the block copolymer layer; the Σ was directly measured with FRES after fracture. The resulting PVP slab was then joined to the PS slab, annealed in a mold at 160 °C for 2 h, and then allowed to cool to room temperature. In this annealing process, some block copolymer chains diffuse away from the interface but most block copolymer chains organize themselves at the interface and approach an equilibrium conformation; i.e., these copolymer chains strengthen the interface between the PS and PVP. The resulting sandwich was then cut with a diamond saw to obtain six strips for the following mechanical fracture toughness measurement. The dimensions of the strips were 50.8 mm long × 8.7 mm wide. The thickness combinations for the PS/PVP samples are 3.0 mm/1.6 mm, 2.3 mm/1.6 mm, 2.0 mm/1.6 mm, 1.6 mm/1.6 mm, 1.6 mm/2.0 mm, 1.6 mm/2.3 mm, and 1.6 mm/3.0 mm, respectively. From Figure 3, the corresponding phase angle ψ's of these specimens are found to be −13, −6, −3, +2.5, +8, +11, and +17°. As mentioned earlier, our previous fracture toughness tests[3,7,8,10] were obtained at fixed phase angle with a thickness ratio of 2.3/1.6, and the phase angle ψ for this geometry is about −6°.

3.3. Fracture Toughness Measurement. The fraction toughness of the interface G_c is given by the critical energy release rate of the interfacial crack. The measurement was performed by inserting a single-edge razor blade, of thickness Δ, at the interface and pushing it into the interface at a constant rate of 3×10^{-6} m/s using a servo-controlled motor drive. The fracture toughness G_c was computed using

$$G_c = \frac{3\Delta^2 E_{PS} h_{PS}^3 E_{PVP} h_{PVP}^3}{8a^4} \times \left[\frac{E_{PS} h_{PS}^3 C_{PVP}^2 + E_{PVP} h_{PVP}^3 C_{PS}^2}{[E_{PS} h_{PS}^3 C_{PVP}^3 + E_{PVP} h_{PVP}^3 C_{PS}^3]^2} \right] \quad (4)$$

where h_{PS} and E_{PS} denote the thickness and the Young's modulus of the PS beam, respectively, and $C_{PS} = 1 + 0.64 h_{PS}/a$;[7] similar quantities are defined for PVP and labeled by the subscript PVP. The crack length a is measured from the crack tip to the edge of the razor blade. To allow many measurements of a, and thus G_c, to be made, the entire history of the crack growth was recorded using a video camera onto a videotape. As mentioned earlier, six specimens were made by cutting six strips from each of the sandwiched plates for each Σ and thickness combination. The error bars reported subsequently for G_c represent ±1 standard deviation of each specimen. At least 16 measurements were made from one specimen. After fracture, the beam thicknesses were measured and were used to calculate G_c and the phase angle ψ accurately.

3.4. Ion Beam Analysis of Fracture Surfaces. After the G_c measurement, the two halves of the fracture surfaces were examined by FRES to determine the density of deuterium atoms on each side and therefore to allow the areal density of dPS blocks of copolymer chains on both the PS and PVP sides (Σ_{PS} and Σ_{PVP}, respectively) to be calculated. The total areal chain density at the interface, Σ, was determined by summing these two measurements.

Details of the ion beam analysis technique can be found in refs 7, 24, and 25 and will not be repeated here.

4. Results

4.1. 800/870 dPS/PVP Block Copolymer. For this block copolymer, whose dPS and PVP blocks are long enough to be well entangled, we examine the effect of the phase angle ψ on the fracture toughness and fracture mechanism for three areal chain densities of block copolymer: $\Sigma = 0.025$, $\Sigma = 0.10$, and $\Sigma = 0.50$ chains/nm^2.

4.1.1. Block Copolymer with $\Sigma = 0.025$ Chains/nm^2. Figure 4a shows the G_c versus ψ curve for the case of $\Sigma = 0.025$ chains/nm^2. For $\psi < 0°$, G_c is very low ($G_c \sim 5$ J/m^2). In comparison, G_c of the bare PS/PVP interface is ~1 J/m^2.[7] Note that for $\psi < 0°$, the crack tip is driven toward the PVP phase, which has a higher crazing stress than the PS. The crazing stresses for PVP and PS under our testing conditions are $\sigma_{d;PVP} = 75$ MPa and $\sigma_{d;PS} = 55$ MPa, respectively.[7] In this regime (low Σ, high N, $\psi < 0°$), it was shown previously by Creton et al.[7] that the interface fails by chain scission. The optical micrograph in Figure 5a shows that the fracture surfaces are very smooth, indicating that no wide crazes are formed at the interface. On the other hand, when $\psi > 0°$, the fracture toughness increases more than 6 times; i.e., $G_c \geq 30$ J/m^2. The transition from low G_c to high G_c occurs sharply at $\psi = 0°$. For $\psi > 0°$, the crack is driven toward the PS phase, which has a lower crazing stress than the PVP phase. In this case, crazes which incline at an angle of approximately 45° from the interface were observed as shown in the optical micrograph in Figure 5b. The formation of these oblique crazes seems to be responsible for the dramatic increase in G_c. These crazes are not continuously formed along the interface as can be seen in Figure 5c. Most of the fractured surface is as smooth as in the case when ψ is negative. This behavior is not surprising as the interface is very weak due to the low copolymer areal chain density. Note that micrographs 5b and 5c are the side view and top view, respectively, of the PS side of the fractured specimen. The bands on the fracture surface (Figure 5c) occur where the oblique crazes in the side view (Figure 5b) intersect that surface. There are corresponding bands on the PVP side of the fractured interface. Occasionally we also observed a wide bundle of oblique crazes formed on the PS side, such as the dark band marked with the arrow in Figure 5d. When the craze bundle formed, the measured fracture toughness was much higher than the typical interfacial fracture toughness we measured at the same interface. The formation of these thicker crazes led to a stick-slip phenomenon; i.e., the crack slows down due to the formation of these thicker crazes and advances suddenly as the crack tip passes the craze bundle region. Under such circumstances, the crack did not advance steadily even though the razor blade was driven at a constant speed.

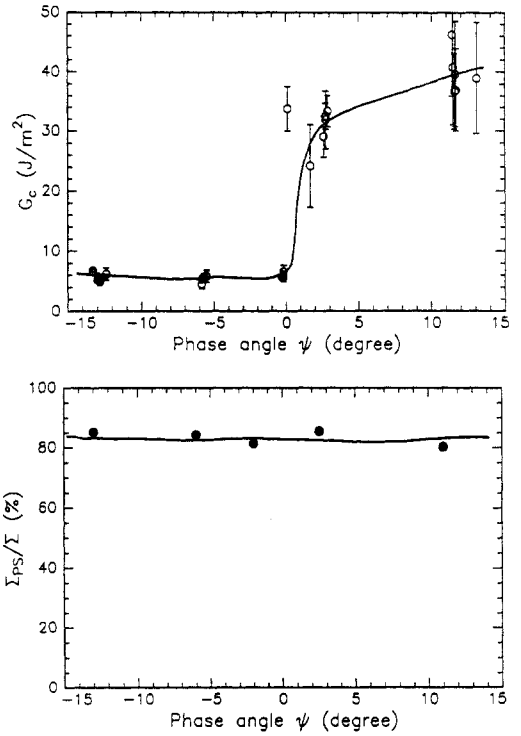

Figure 4. (a, top) Fracture toughness G_c as a function of phase angle ψ for areal chain density $\Sigma = 0.025$ chains/nm^2 of the 800/870 dPS/PVP block copolymer. (b, bottom) Fraction of dPS block on the PS side of the fractured surface, Σ_{PS}/Σ, as a function of phase angle ψ for $\Sigma = 0.025$ chains/nm^2 of the 800/870 dPS/PVP block copolymer.

Since the chain density Σ is small, the copolymer chains bridging the PS/PVP interface will break before a stable nonoblique craze forms with its tip on the interface. Figure 4b shows the fraction of block copolymer chains found on the PS side, i.e., Σ_{PS}/Σ, as a function of ψ. More than 80% of the deuterium was found on the PS side, indicating that the majority of the interface still fails by scission of the block copolymer chains which were broken near the dPS/PVP joint. If a craze forms along the interface in the PS, it fractures where the dPS block brush penetrates into the PS homopolymer, leaving only 10% of the deuterium on the PS side.[7]

4.1.2. 800/870 Block Copolymer with $\Sigma = 0.10$ Chains/nm^2. Figure 6a shows that G_c ranges from a minimum of 50 J/m^2 for $-10 < \psi < 0°$ to values of 170 J/m^2 for $\psi \approx 5°$ and 100 J/m^2 for $\psi \approx -15°$. Unlike the case of $\Sigma = 0.025$ chains/nm^2, crazes which incline at an angle of approximately 135° to the crack propagation direction into the PS are observed (see Figure 7a) for negative phase angles. The oblique crazes at large negative ψ are closely spaced. The increase in fracture toughness for $\psi < -10°$ may be due to the thickening of these oblique crazes.

For samples with positive phase angles, the fracture toughness G_c increases rapidly as ψ increases from zero to

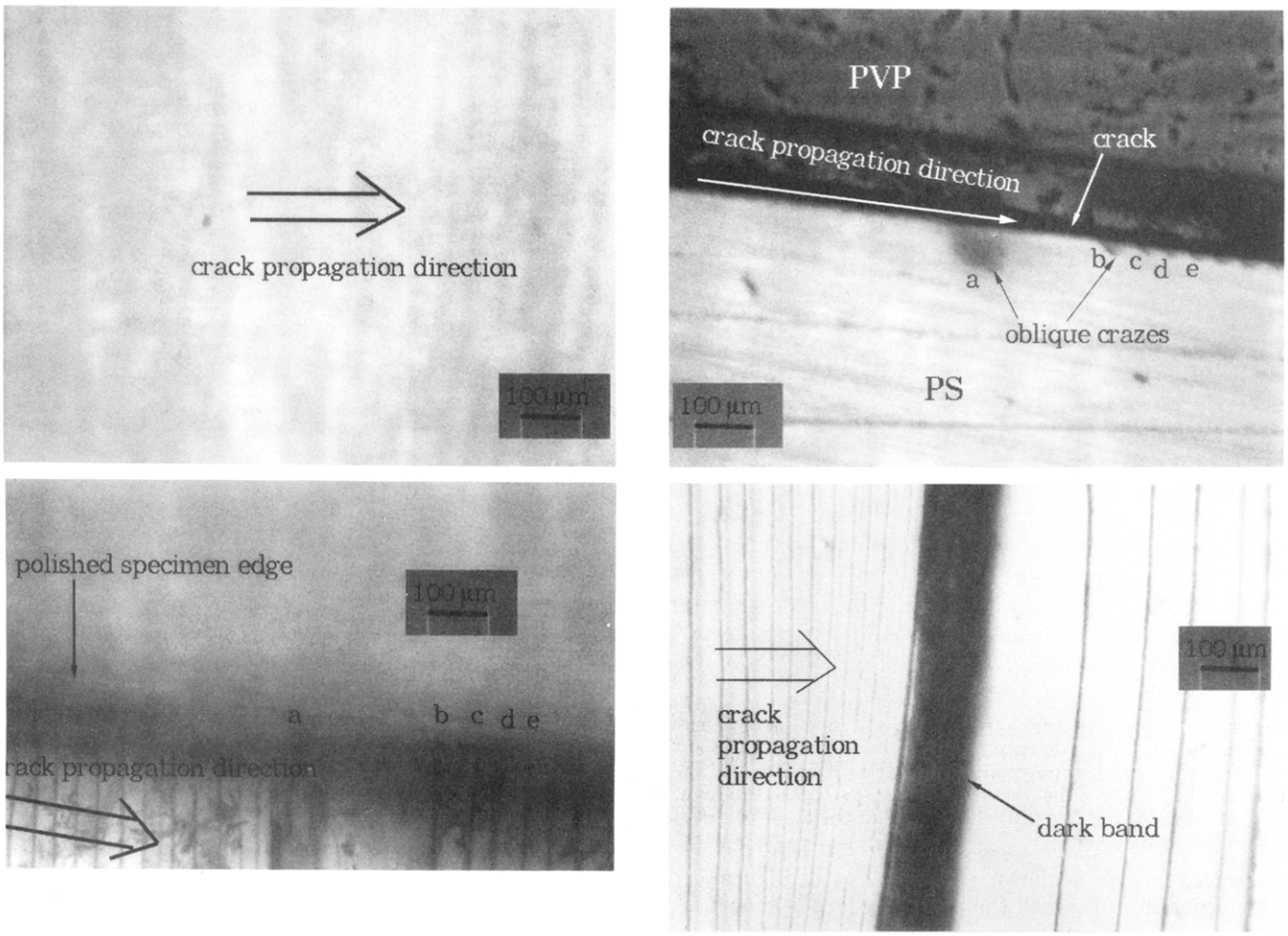

Figure 5. Some optical micrographs of interfaces reinforced by the 800/870 block copolymer with an areal chain density $\Sigma = 0.025$ chains/nm^2. (a, top left) Top view of the fracture surface (PS side) for $\psi < 0°$. There are no oblique crazes observed for this negative phase angle case. The fracture surface is very smooth. (b, top right) Side view of the fractured interface ($\psi > 0°$). There is a one to one correspondence between the oblique crazes in this side view picture and the bands on the fracture surface in Figure 5c. (c, bottom left) Top view of the PS side of the fractured interface ($\psi > 0°$). (d, bottom right) Another top view of the PS side of the fractured interface ($\psi > 0°$). The dark band indicated by the arrow corresponds to a wide bundle of crazes where the crack tip stopped during stick-slip crack propagation.

small positive values, e.g., a 3-fold increase in fracture toughness (from 50 to 150 J/m^2) in less than 5°. A change in phase angle from 0 to 5° corresponds to a change in thickness ratio from 0.9 to 1.1. In contrast to the 135° oblique crazes observed for negative phase angles, crazes which incline at an angle of approximately 45° from the crack propagating direction are observed for positive phase angles. These crazes are shown in Figure 7b. In this case, the oblique crazes are much more closely spaced and longer compared to those at lower areal chain density ($\Sigma = 0.025$ chains/nm^2 and $\psi > 0°$) and those at the same areal chain density but with $\psi < 0°$. The increase in fracture toughness for $\psi > 0°$ may be due to the thickening and elongation of these oblique crazes.

Our test data are limited to specimens with $\psi < 5°$. Attempts to increase the phase angle beyond 5° resulted in the interface crack propagating off the interface, causing cohesive failure of the PS slab even though the interface fracture toughness at this phase angle is still smaller than that of the bulk PS, which is about 400 J/m^2.

In addition to the oblique crazes just discussed, a craze ahead of the crack tip can also form with its tip on, or close to, the interface at this higher areal chain density. Figure 6b shows the fraction of block copolymer chains found on the PS side. Our FRES data show that most of the dPS block of the block copolymer chains is found on the PVP side of the fracture surface. Thus, the failure mechanism in this case corresponds to the breakdown of the crazes in the PS side of the interface.

An argument can be made that despite their importance for fracture toughness at the extremes of ψ (i.e., $\psi > 0°$ or $\psi < -10°$), the oblique crazes do not greatly affect the final fracture mechanism at the interface, which still involves breakdown of a craze lying along the interface ahead of the crack in the region where the dPS block brush and the PS homopolymer interpenetrate. For $-10 < \psi < 0°$, it seems very unlikely that the oblique crazes running at 135° affect the fracture path, since the crack would have to propagate "backward" into these oblique crazes. But then the fact that the same fraction $\Sigma_{PS}/\Sigma = 10\%$ of dPS on the PS side is seen for not only $-10 < \psi < 0°$ but also $\psi < -10°$ and $\psi > 0°$ (Figure 6b) strongly suggests that the oblique crazes do not much affect the fracture path in these cases either. For example, for $\psi > 0°$, one might suspect that the 45° oblique crazes might cause the crack to propagate in craze matter further from the interface than for $\psi < 0°$, thus resulting in almost no dPS on the PS side of the fracture. That the fraction of dPS on the PS side remains constant, or even increases slightly at $\psi > 0°$, indicates that such a hypothesis is unlikely to be true.

4.1.3. 800/870 Block Copolymer with $\Sigma = 0.50$ Chains/nm^2. The high areal chain density results in the formation of a lamellar block copolymer structure at the

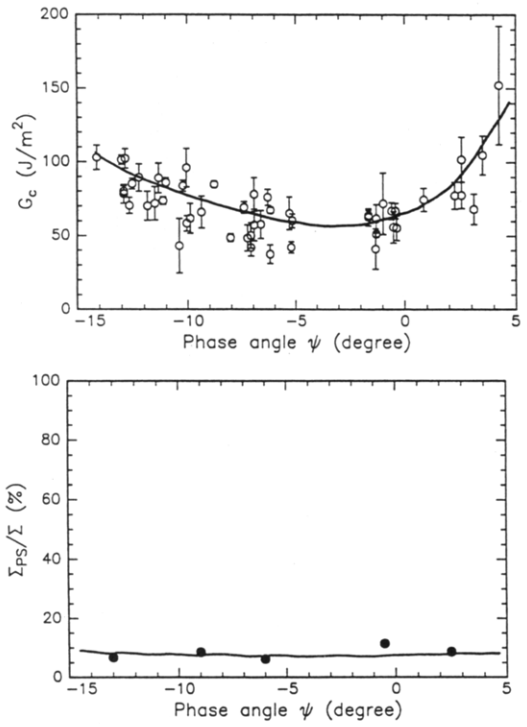

Figure 6. (a, top) Fracture toughness G_c as a function of phase angle ψ for areal chain density Σ = 0.10 chains/nm^2 of the 800/870 dPS/PVP block copolymer. (b, bottom) Fraction of dPS block on the PS side of the fractured surface, Σ_{PS}/Σ, as a function of phase angle ψ for Σ = 0.10 chains/nm^2 of the 800/870 dPS/PVP block copolymer.

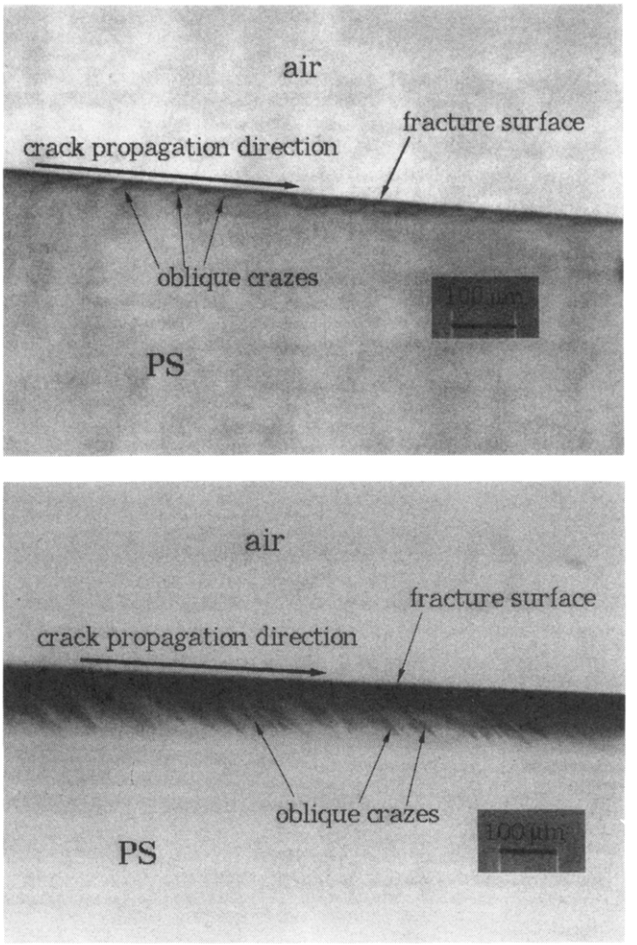

Figure 7. Some optical micrographs of interfaces reinforced with a larger areal chain density Σ = 0.10 chains/nm^2 of the 800/870 dPS/PVP block copolymer. (a, top) Side view of the fractured interface ($\psi < 0°$). The oblique crazes form at an angle of 135° to the crack propagation direction ($\psi = -10°$). (b, bottom) Side view of the fractured interface ($\psi > 0°$). The oblique crazes form at an angle of 45° to the crack propagation direction (ψ = 5°).

interface,[10] which is shown schematically in Figure 8a. The variation of G_c with the phase angle ψ is shown in Figure 9a. The transition from low to high fracture toughness occurs around −9° instead of near 0°. Note that, as pointed out by Washiyama et al.,[10] the fracture toughness in this case is actually lower than the previous case of Σ = 0.10 chains/nm^2 (cf. Figure 6); i.e., G_c does not necessarily increase monotonically with Σ.

Like the fracture toughness, the fraction of block copolymer chains found on the PS side, Σ_{PS}/Σ, also has a transition at ψ = −9°, as shown in Figure 9b. This phenomenon can be explained as follows. The PS lamella is weaker than the bulk material due to the diffusion of low molecular weight homopolymers into the lamella.[10] When the crack was driven with a negative phase angle $\psi < -9°$, the craze zone ahead of the crack tip propagated in the PS lamella since the applied stress tends to drive the crack to the PVP side. The PVP homopolymer as well as the PVP lamella has a higher crazing stress, so the craze tip was trapped in the PS lamella, and 135° oblique crazes, if formed, cannot penetrate the more craze resistant PVP lamella and propagate into the PS homopolymer. As a partial check on this hypothesis, we note that the location of the deuterated PS block is (1) along the bulk PS homopolymer/PVP lamella interface and (2) in the PS lamella (see Figure 8b). If craze breakdown occurs in the PS lamella, the majority of the deuterium should be found on the PS side. For example, $\Sigma_{PS}/\Sigma \sim {}^2/_3 = 0.67$ if the craze fails in the middle of the PS lamella and should decrease to a lower value as the crack or craze tip moves toward the bulk PS as the phase angle increases. This behavior is confirmed by our FRES results shown in Figure 9b. Since the PS lamellar layer is weaker than the dPS brush/PS bulk homopolymer interface,[10] the observed G_c is lower than the previous case of Σ = 0.10 chains/nm^2.

It is plausible that, as the value of ψ increases from −9° so that the tendency for the crack to grow toward the PVP phase is reduced, sufficiently long oblique crazes can form which penetrate the PVP lamella and grow into the bulk PS. The existence of these oblique crazes could lead to the observed higher fracture toughness. These oblique crazes can also give rise to local damage in the PVP lamella so that the crack tip in the PS lamella can occasionally penetrate the PVP lamella and propagate along the homopolymer/PVP lamella interface, thus forming a craze on the interface extending into the bulk PS. This excursion allows the craze to grow in the bulk PS, leading to a further increase in fracture toughness. The oscillation of the craze and crack from one interface in the lamella to another will leave more dPS on the PVP side (see Figure 8c) and was observed directly at ψ = −6°.[10] The deuterium found on the PS side should therefore decrease as ψ increases from −9° and such a decrease was observed in the FRES results (Figure 9b). Unfortunately, we did not observe these specimens using the optical microscope, so it is not possible for us to confirm the existence of oblique crazes in this case. Clearly, any oblique crazes inside the PS lamella, if they exist, would be too small to be observed using optical microscopy. However, if any oblique crazes penetrate through the PVP lamella into the bulk PS, then it may be possible to observe them.

4.2. 510/540 Block Copolymer with Σ = 0.50 Chains/nm^2. The effect of 510/540 block copolymer was examined in the lamellar regime to confirm our previous observations

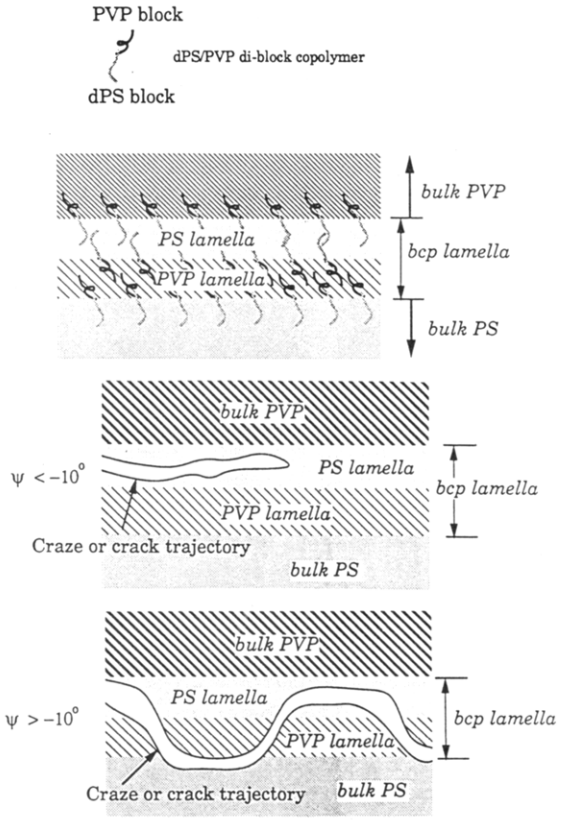

Figure 8. (a, top) Schematic of the lamellar structure of the 800/870 block copolymer at the interface for the high areal chain density ($\Sigma = 0.5$ chains/nm^2). (b, middle) Craze or crack trajectory trapped in the PS lamella at large negative ψ. (c, bottom) Craze or crack trajectory which penetrates through the PVP lamella at small negative or positive ψ.

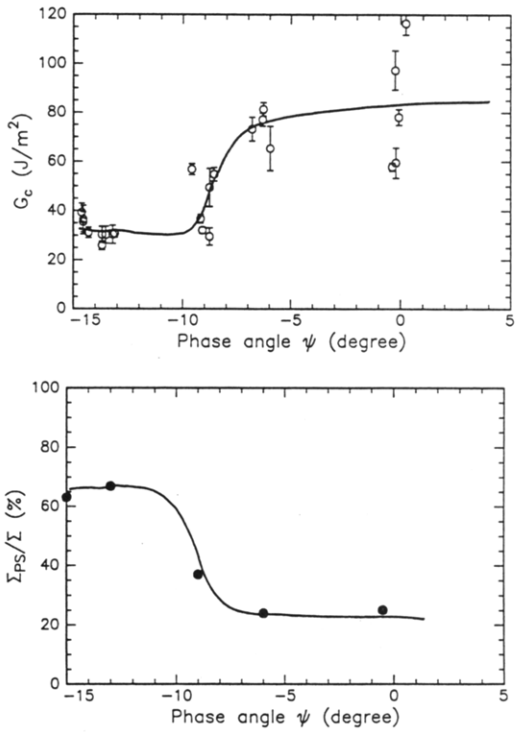

Figure 9. (a, top) Fracture toughness G_c as a function of phase angle ψ for areal chain density $\Sigma = 0.50$ chains/nm^2 of the 800/870 dPS/PVP block copolymer. (b, bottom) Fraction of dPS block on the PS side of the fractured surface, Σ_{PS}/Σ, as a function of phase angle ψ for $\Sigma = 0.50$ chains/nm^2 of the 800/870 dPS/PVP block copolymer.

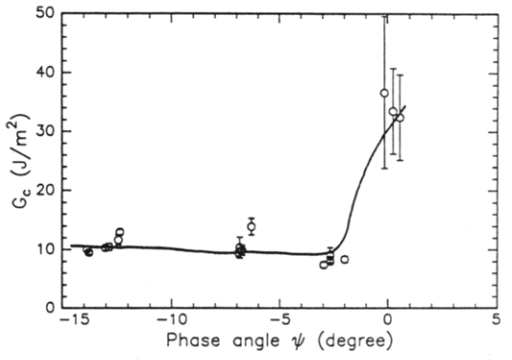

Figure 10. Fracture toughness G_c as a function of phase angle ψ for areal chain density $\Sigma = 0.50$ chains/nm^2 of the 510/540 dPS/PVP block copolymer.

(800/870, $\Sigma = 0.50$ chains/nm^2). The results shown in Figure 10 are similar to those in Figure 9a for the 800/870 block copolymer. The PS lamella is weaker than the one in the 800/870 system due to the shorter dPS block, so it is easier for the crack to propagate in the PS lamella. As a consequence, the craze and crack are trapped in the PS lamella as long as the phase angle tends to drive the crack into the PVP. This is the reason why the G_c transition occurs between $\psi = 0°$ and $\psi = -2°$, which is a much larger phase angle than that, $\psi = -9°$, required for the transition in the 800/870 block copolymer.

4.3. 580/220 dPS/PVP Block Copolymer. In this case the PVP block of the block copolymer is shorter than the entanglement length $N_e = 255$, so the PVP block can be pulled out of the PVP bulk phase at the interface at sufficiently low areal chain densities. Since the interface is weaker than that of the 800/870 system, experimental data can be obtained up to a phase angle of 18°. The asymmetry of the dPS and PVP block lengths means that at large Σ, beyond the value ~0.2 chains/nm^2, corresponding to saturation of the block copolymer at the interface, the excess block copolymer forms spherical micelles off the interface in preference to lamellae. Unlike the lamellar structure in the previous cases, these micelles do not affect the toughness of the interface.[7,8] Two areal chain densities, 0.04 and 0.15 chains/nm^2, of this block copolymer were examined in detail.

4.3.1. 580/220 Block Copolymer with $\Sigma = 0.04$ Chains/nm^2. The fracture toughness G_c vs phase angle ψ curve for the 580/220 block copolymer with $\Sigma = 0.04$ chains/nm^2 is similar to that for the 800/870 block copolymer with $\Sigma = 0.025$ chains/nm^2 (cf. Figure 4). G_c is about 3 J/m^2 for $\psi < 0°$. According to previous experiments,[7,8] the weak interface fails by pull-out of the PVP block before a stable craze can be formed. Figure 11b shows the fraction of block copolymer chains found on the PS side of the interface after fracture, i.e., Σ_{PS}/Σ, as a function of ψ. Almost 100% of the deuterium was found on the PS side, which substantiates our hypothesis that the copolymer chains are pulled out from the PVP side of the interface. As in the case of the 800/870 system with $\Sigma = 0.025$ chains/nm^2 (see 4.1.1), we observed oblique crazes inclined at an angle of 45° away from the interface for $\psi > 0°$, and crack growth occurred in a stick-slip manner. Figure 11a shows that an 8-fold increase in fracture toughness occurs when the phase angle increases from −1 to +2°. After the sharp transition, the fracture toughness increases as a function of phase angle. The FRES results in Figure 11b show that the failure mechanism, which now must involve formation of a craze (or crazes) ahead of the crack, is still chain pull-out for positive phase angles.

4.3.2. 580/220 Block Copolymer with $\Sigma = 0.15$ Chains/nm^2. Due to the short PVP block of the block

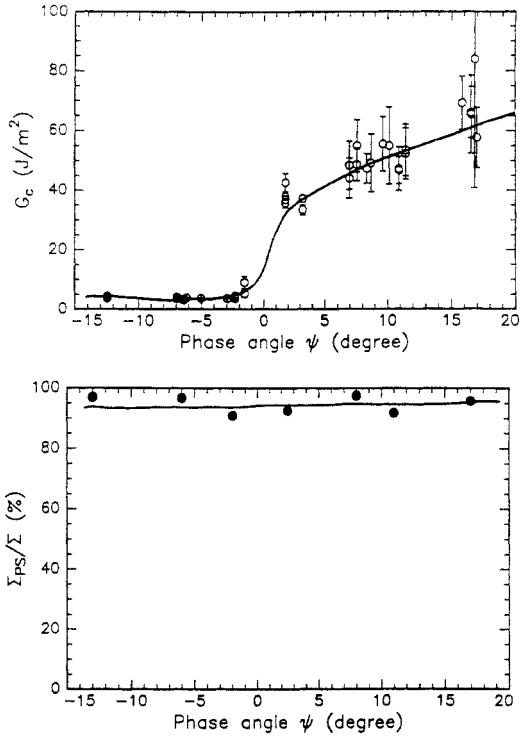

Figure 11. (a, top) Fracture toughness G_c as a function of phase angle ψ for areal chain density Σ = 0.04 chains/nm^2 of the 580/220 dPS/PVP block copolymer. (b, bottom) Fraction of dPS block on the PS side of the fractured surface, Σ_{PS}/Σ, as a function of phase angle ψ for Σ = 0.04 chains/nm^2 of the 580/220 dPS/PVP block copolymer.

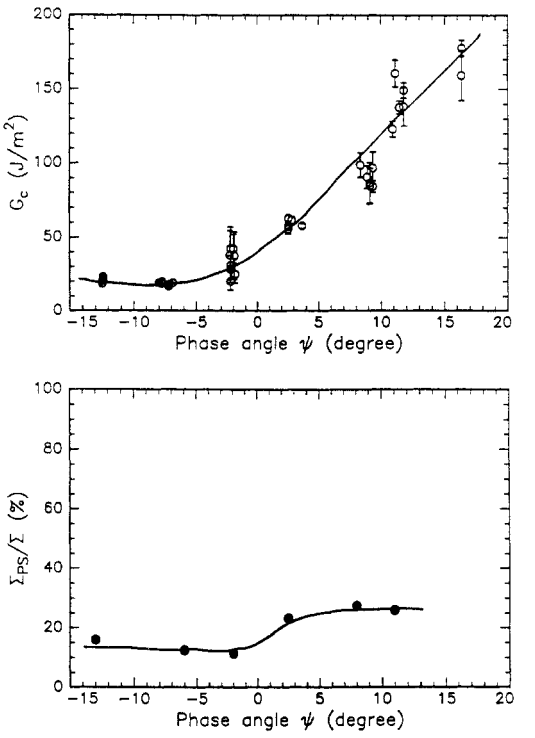

Figure 12. (a) Fracture toughness G_c as a function of phase angle ψ for areal chain density Σ = 0.15 chains/nm^2 of the 580/220 dPS/PVP block copolymer. (b, bottom) Fraction of dPS block on the PS side of the fractured surface, Σ_{PS}/Σ, as a function of phase angle ψ for Σ = 0.15 chains/nm^2 of the 580/220 dPS/PVP block copolymer.

copolymer, the interface is not strong enough to allow wide crazes to grow so that for large negative phase angles, no stable crazes can form in the PVP side but a stable thin craze with its tip on the interface is expected to form on the PS side.[7,8] For samples with positive phase angles, oblique crazes are observed on the PS side which are inclined at an angle of approximately 45° to the interface. The transition from low to high toughness occurs near −2°, which corresponds to a specimen thickness of 1.6 mm for PVP and 2.0 mm for PS. At this phase angle, the oblique crazes can be inclined in either 45° or 135° directions depending on the local chain density and the surface flatness. Crack growth proceeds in a stick-slip manner as described earlier so that the crack length in the evaluation of the fracture toughness is not very well defined. These observations could explain the relatively large spread in the G_c data at $\psi = -2°$. When $\psi > 3°$, the oblique crazes are formed at much closer intervals along the interface and appear continuous on a macroscopic scale. For very large phase angles, the crack propagates away from the interface, resulting in the cohesive failure of the PS slab.

With the increase in Σ from 0.04 to 0.15 chains/nm^2, the failure mechanism shifts from chain pull-out to crazing followed by craze breakdown in the PS homopolymer and copolymer brush over the entire range of ψ. Due to the short PVP chains, the craze breakdown in the brush is accompanied by some chain pull-out from the PVP side.[8] This picture is confirmed by the FRES results in Figure 12b, which show that most of the dPS block of the block copolymer chains was found on the PVP side of the fracture surface, indicating that most of the breakdown occurs at the dPS brush/PS homopolymer interface as before. A larger fraction of dPS (15–30%) is found on the PS side than for the block copolymer 800/870 with the larger PVP block (5–10%; cf. Figure 6b).

5. Discussion

Our experimental results indicate that any fracture toughness greater than 10 J/m^2 is primarily due to the formation of crazes. Typically, for weak interfaces (e.g., 800/870 block copolymer with Σ = 0.025 chains/nm^2 and 580/220 block copolymer with Σ = 0.04 chains/nm^2) no crazes were observed until the phase angle became positive. Crazing was observed along interfaces with no block copolymer reinforcement as long as the crack was loaded with a positive phase angle.[5,7] A natural question is: why does crazing occur since the fracture toughness of the interface is much lower than that of the fracture toughness of the bulk PS homopolymer? A related problem is that the direction of crack growth in general does not necessarily coincide with the interface where the fracture toughness is much lower than that of the bulk homopolymer. For example, for strong interfaces ($G_c \geq 150$ J/m^2), the crack strays from the interface, leading to cohesive failure of the PS slab when the phase angle exceeds 5°. Therefore, the formation of crazes and the crack growth trajectory cannot be predicted based solely on the relative fracture toughness of the bulk homopolymers and the interface. For example, the fact that the interface has a much lower fracture toughness than the bulk homopolymer does not necessarily mean that the stress required to initiate a craze with its tip on the interface is smaller than that to initiate a craze with its tip in the bulk polymer. Crack growth, however, need not be in the direction of the oblique crazes. A thin craze can still be formed at the interface and will break down there so that crack growth will occur along the interface as long as the interface is less tough than the bulk homopolymer. Our experimental results seemed to confirm this hypothesis. On the other hand, when the interface is sufficiently strong and the phase angle is sufficiently positive (e.g., in the case of the 800/870 system with Σ = 0.1 chains/nm^2 and $\psi = 5°$), crack growth is likely

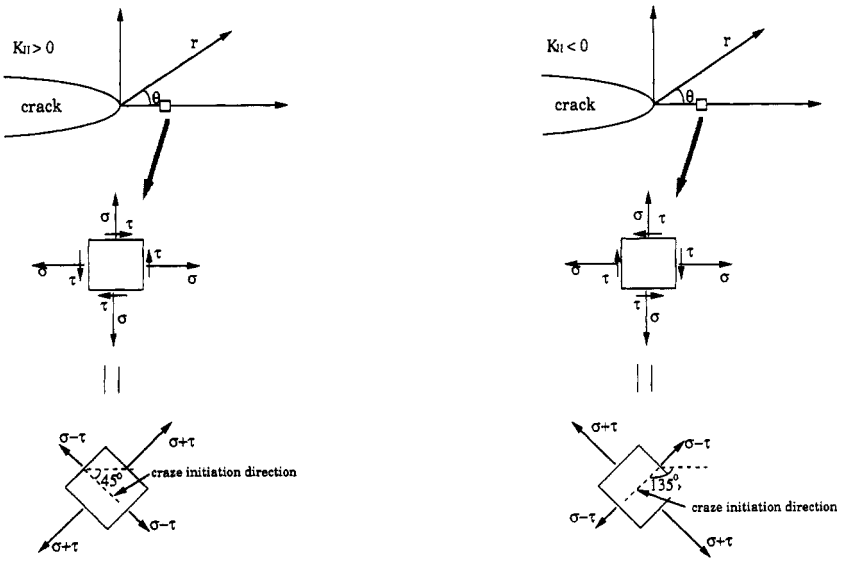

Figure 13. (a, left) Stress state directly ahead of a crack tip at $\theta = 0°$ for $K_{II} > 0$. (b, right) Stress state directly ahead of a crack tip at $\theta = 0°$ for $K_{II} < 0$.

to occur in the direction of the oblique craze so that cohesive failure of the PS occurs.

To explain the initiation of the oblique crazes, consider the stress state near the tip of the interface crack, i.e.

$$\sigma_{kl} = f_{kl}(K,r,\theta,\epsilon) \qquad k,l = 1,2 \tag{5}$$

where r,θ is a polar coordinate system centered on the crack tip, which is the origin. $K = K_1 + iK_2$ is the complex stress intensity factor, and f_{kl} are universal functions describing the stress distribution for given material pairs.[19]

The stress state ahead of the crack tip can be understood by considering the special case of $\epsilon = 0$, which is a very good approximation for the PVP/PS materials in our experiments ($\epsilon = -2.8 \times 10^{-3}$). Directly ahead of the crack tip at $\theta = 0°$, for positive phase angles, the maximum principal tensile stress acts normal to a plane oriented at about 45° to the crack propagation direction as shown in Figure 13a. However, for negative phase angles, the maximum principal tensile stress occurs on a plane oriented at about 135° as shown in Figure 13b. The direction of maximum principal tensile stress at a point on the interface changes its orientation by 90° as the phase angle increases from negative to positive. In this case, a zero phase angle (i.e., $K_2 = K_{II} = 0$) implies that the in-plane stress state near the crack tip is purely hydrostatic (i.e., $\sigma_{xx} = \sigma_{yy}$ and $\sigma_{xy} = 0$). Thus a small positive phase angle or $K_{II} > 0$ will orient the principal maximum tensile stress at $\theta = 0°$ to act on a plane inclined at 45° (Figure 13a). If a craze were to initiate normal to the direction of maximum principal tensile stress, then it should be inclined at angle of approximately 45°. On the other hand, $K_{II} < 0$ will orient the maximum principal tensile stress at $\theta = 0°$ to act on a plane inclined at 135° (Figure 13b), so that crazes are inclined along the 135° direction when the phase angle is negative. One may, however, argue that the direction of the principal tensile stress at a material point directly ahead of the crack tip may be influenced by the higher order terms of the series expansion of which eq 5 is the first and dominant term. A finite element calculation using the exact specimen geometry showed that, for a PVP/PS ADCB specimen with a positive phase angle of 8°, the maximum principal direction is 42° at a distance of about 10 μm from the crack tip. Therefore, eq 5 can be used to estimate the principal directions for $r < 10$ μm.

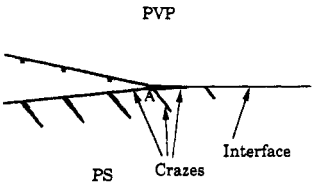

Figure 14. Schematic of craze initiation at the interface near the tip of the craze for $\psi > 0°$.

It should also be noted that the maximum principal tensile stress at a given radius r from the crack tip does not occur at $\theta = 0°$. However, the craze still may initiate directly ahead of the interface crack tip from the interface since the material is less homogeneous and weaker there. Thus, it is possible that a craze can be formed at $\theta = 0°$ in the direction of 45 or 135°. If ϵ is nonzero, then the maximum principal stress direction at $\theta = 0°$ may deviate from 45°.

If a craze initiates directly from the tip of a crack which is blunted with a very small root radius (by, for example, the meniscus instability mechanism[29]), $\sigma_{xx} = 0$ and σ_{yy} is large there and the craze will grow along a plane $\theta = 0$ if $\psi = 0$ or along a plane where $\sigma_{r\theta} = 0$ if $\psi \neq 0$. However, if a craze initiates from the interface at a distance greater than the radius of the tip of the blunted crack ahead of the crack tip, the above discussion should accurately predict the craze growth direction. The oblique craze observed therefore must initiate somewhere ahead of the crack tip, not directly at it.

The formation of oblique crazes does not necessarily mean that a craze cannot be formed along the interface (i.e., the tip of this craze is on or close to the interface). Our FRES results are consistent with such a formation. A possible scenario is shown in Figure 14 where a small craze with its tip on the crack line lies above the oblique craze. The shorter craze which lies on the interface cannot grow until the oblique craze thickens sufficiently so that the stress concentration at the point A becomes high enough to break the interface next to the short craze, thus leading to the growth of the crack and more crazing along the interface. The crack propagation leads to more oblique crazes and the process continues. Another way of justifying the above hypothesis is to consider a recent calculation of Hui et al.[30] They considered the problem of a single oblique craze initiated at an interface crack tip. This calculation showed an oblique craze inclined at an angle of 45° with

respect to the interface corresponded to an applied phase angle of about 40°, which is much larger than the phase angle of a few degrees we applied in our experiments. This result also implies that the oblique crazes do not grow directly from the crack tip but as secondary crazes somewhere ahead of it.

Finally, we notice that oblique crazes associated with negative phase angles which oriented at about 135° to the crack propagation direction are much shorter than the oblique crazes that are formed under positive phase angles because the stress state favors the opening up of the latter.

We note that the formation of crazes at the interface was also observed by Brown[5] in his experiments on PS/PMMA (poly(methyl methacrylate)) interfaces. In his experiment, the interface between the incompatible PS and PMMA was reinforced by a thin layer of PS–PMMA diblock copolymer. Brown found that when the interface crack was driven toward PS, oblique crazes were observed in the PS layer. Cho et al. also found that some of the PS craze material remained on the PMMA side of the interface after fracture.[31] It is interesting to note that Brown does not mention the existence of 135° oblique crazes when the system is loaded with a negative phase angle.

Our experimental results differ from previous TEM experimental observations obtained on thin microtomed films of the same system.[11] Washiyama et al.[11] did not notice any oblique crazes at the interfaces in these films. The stress state ahead of the crack tip in the microtomed film ($\sim$0.5 μm in thickness) is much closer to plane stress than that ahead of the crack tip in the center of the ADCB specimen which is nearly that of plane strain. The plane strain condition gives rise to higher hydrostatic stress (about 33% more if Poisson's ratio is $\nu = 0.33$ since $\sigma_{zz} = \nu(\sigma_{xx} + \sigma_{yy})$ in plane strain). The resulting elevation of hydrostatic stress may be crucial to the initiation of the oblique crazes. In support of this hypothesis, it should be noted that the oblique crazes did not form along the interface at the free surface of the ADCB specimen but only at a distance of some tens of micrometers below the surface. Our optical micrographs were obtained by polishing down from the free surface of the sample until oblique crazes were visible.

6. Conclusions

The effect of phase angle ψ on the interface fracture toughness G_c of planar interfaces between PS and PVP, which were reinforced with dPS/PVP block copolymers, was investigated by varying the thickness ratio of PS and PVP beams in an ADCB specimen. At low areal chain densities of the block copolymer where the interface was weak, dramatic changes in G_c occurred in a very narrow range of phase angle. These dramatic changes are related to the formation of widely spaced oblique crazes along the interface initiated ahead of the crack tip and may result in the crack growing in a stick-slip fashion.

When the interface was reinforced with high areal chain densities of block copolymer, the interface was strong and more and longer oblique crazes formed along the interface. For these high-G_c cases, oblique crazes were formed at 45° to the crack propagation direction for $\psi > 0°$ and 135° for $\psi < 0°$. However, only the 45° oblique crazes are favored to grow due to the crack tip stress field. The growth of these oblique crazes contributes to the high G_c values for the $\psi > 0°$ cases. For small $\psi < 0°$ cases, we believe that these oblique crazes do not contribute significantly to the measured fracture toughness G_c.

For the interfaces reinforced by symmetric block copolymers, adding an excess of block copolymer over that required to saturate the interface led to the formation of block copolymer lamellae. Changing the phase angle alters the craze and crack trajectory in the lamellar layer, which causes large changes in G_c.

Our FRES result revealed that the local failure mechanisms at the crack tip, namely, chain pull-out, chain scission, and craze breakdown, are not affected by changes in the phase angle as long as the crack growth occurs along the interface.

Acknowledgment. We gratefully acknowledge that this work was carried out as part of a project of the Cornell Materials Science Center (MSC), which is funded by the National Science Foundation, and benefited from the use of the MSC Central Facilities. J.W. is supported by a grant from Showa Denko K.K., Japan.

References and Notes

(1) Fayt, R.; Jérôme, R.; Teyssié, Ph. *J. Polym. Sci., Polym. Phys. Ed.* **1989**, *27*, 775.
(2) Fayt, R.; Teyssié, Ph. *Polym. Eng. Sci.* **1989**, *29*, 538.
(3) Creton, C.; Kramer, E. J.; Hadziioannou, G. *Macromolecules* **1991**, *24*, 1846.
(4) Cao, H. C.; Dagleish, B. J.; Evans, A. G. *Closed Loop* **1990**, *23*, 3929.
(5) Brown, H. R. *J. Mater. Sci.* **1990**, *25*, 2791.
(6) Brown, H. R. *Macromolecules* **1989**, *22*, 2859.
(7) Creton, C.; Kramer, E. J.; Hui, C. Y.; Brown, H. R. *Macromolecules* **1992**, *25*, 3075. Creton, C. Ph.D Thesis, Cornell University, Ithaca, NY 1992.
(8) Washiyama, J.; Kramer, E. J.; Hui, C. Y. *Macromolecules* **1993**, *26*, 2928.
(9) Smith, J. W.; Kramer, E. J.; Xiao, F.; Hui, C. Y.; Reichert, W.; Brown, H. R. *J. Mater. Sci.* **1993**, *28*, 4234.
(10) Washiyama, J.; Creton, C.; Kramer, E. J.; Xiao, F.; Hui, C. Y. *Macromolecules* **1993**, *26*, 6011.
(11) Washiyama, J.; Creton, C.; Kramer, E. J. *Macromolecules* **1992**, *25*, 4751.
(12) Shull, K. R.; Kramer, E. J.; Hadziioannou, G.; Tang, W. *Macromolecules* **1990**, *23*, 4780.
(13) Shull, K. R.; Kramer, E. J. *Macromolecules* **1990**, *23*, 4769.
(14) Dai, K. H.; Kramer, E. J.; Shull, K. R. *Macromolecules* **1992**, *25*, 220.
(15) Xu, D. B.; Hui, C. Y.; Kramer, E. J.; Creton, C. *Mech. Mater.* **1991**, *11*, 257.
(16) England, A. H. *J. Appl. Mech.* **1965**, *32*, 400.
(17) Erdogan, F. *J. Appl. Mech.* **1965**, *32*, 403.
(18) Rice, J. R.; Sih, G. C. *J. Appl. Mech.* **1965**, *32*, 418.
(19) Rice, J. R. *J. Appl. Mech.* **1988**, *55*, 98.
(20) Suo, Z.; Hutchinson, J. W. Mater. *Sci. Eng.* **1990**, *A107*, 135.
(21) Charalambides, P. G.; Lund, J.; Evans, A. G.; McMeeking, R. M. *J. Appl. Mech.* **1991**, *56*, 77.
(22) Suo, Z.; Hutchinson, J. W. *Int. J. Fract.* **1990**, *43*, 1.
(23) Xiao, F.; Hui, C. Y.; Kramer, E. J. *J. Mater. Sci.* **1993**, *28*, 5620.
(24) Feldman, L. C.; Mayer, J. W. In *Fundamentals of Surface and Thin Film Analyses*; North-Holland: Amsterdam, 1986.
(25) Mills, P. J.; Green, P. F.; Palmstrom, C. J.; Mayer, J. W.; Kramer, E. J. *J. Appl. Phys. Lett.* **1984**, *45*, 958.
(26) Shull, K. R. Ph.D Thesis, Cornell University, Ithaca, NY, 1990.
(27) Hui, C. Y.; Ruina, A.; Creton, C.; Kramer, E. J. *Macromolecules* **1992**, *25*, 3948.
(28) Kramer, E. J. *Adv. Polym. Sci.* **1983**, *52/53*, 1.
(29) Argon, A. S.; Salama, M. M. *Mater. Sci. Eng.* **1977**, *23*, 219.
(30) Hui, C. Y.; Xiao, F.; Kramer, E. J. *Compos. Mater. Struct., ASME Proc.* **1993**, *AD-Vol. 37, AMD-Vol. 179*, 269.
(31) Cho, K.; Brown, H. R.; Miller, D. C. *J. Polym. Sci., Polym. Phys. Ed.* **1990**, *28*, 1699.